A study of a micro-indentation technique for estimating the fracture toughness of Al6061-T6

Sina Amiri*, Nora Lecis, Andrea Manes, Marco Giglio

Politecnico di Milano, Department of Mechanical Enigneering, via La Masa 1, 20156 Milano, Italy

Article history:
Received 6 May 2013
Received in revised form 30 July 2013
Accepted 19 October 2013
Available online 28 October 2013

1. Introduction

Among the different types of failure such as buckling and excessive plastic deformation, fracture failure is one of the challenging structural damages, to be considered in the design and evaluation of mechanical components in industrial applications. In general, fracture starts from a crack, a notch or a flaw. Fracture toughness, which expresses the resistance of material to crack growth, is a very important parameter in many engineering applications to assess and design the structural integrity of components under extreme and ultimate load (Giglio et al., 2012). There are some standard measurement methods which can be followed to determine it, such as the ASTM standard E399 and E1820. These standards are quite complex and time consuming in terms of fixture design, pre-cracking process, etc. They have severe limitations in terms of the specimen requirements which can practically cause difficulty for very small components. Thus, finding an alternative method to measure fracture toughness in a non-destructive way is very useful especially in industrial applications, where fracture toughness can be measured on final components.

An indentation test, as an advanced version of a conventional hardness test, is widely used in structural applications and in various engineering research fields. Since indentation tests are relatively easy to implement in a non-destructive manner and provide an array of information about the material under investigation, there are several studies to evaluate the behaviour of materials by this technique. Considerable research efforts have been undertaken to probe the elastic and plastic properties of different materials with this technique (Xu and Chen, 2010; Giannakopoulos and Suresh, 1999; Yonezu and Chen, 2010; Ogasawara et al., 2009; Cao and Lu, 2004; Luo and Lin, 2007) due to the little sample preparation required and its application potential in macro-to nano-scales. These approaches are at present quite consolidated and have been standardized such as the ISO/TR 29381.

Recently the instrumented micro-indentation is used to study the local elastoplastic properties of nickel base super-alloys that has been widely used for fabrication of key load-carrying components in steam turbines that usually undergo a typical combination of alternating loading and elevated temperature exposure in practical service conditions (Takagi et al., 2004; Ye et al., 2012). The local mechanical properties are tested by using micro-indentation technique also in the welding process of aluminium alloys (Ambriz et al., 2011) as well as to indicate time dependent material degradation on Cr–Ni (Mo) heat-resistant steels for facilities in petrolchemical and power plants (Jang et al., 2005).

* Corresponding author. Tel.: +39 02 2399 8668; fax: +39 02 2399 8263.
E-mail address: sina.amiri@polimi.it (S. Amiri).

However, fracture mechanics is another important aspect which can be exploited by means of the micro-indentation technique. At present research focuses on the estimation of fracture toughness of brittle materials by this technique (Maerky et al., 1996; Zhang et al., 2010; Lawn et al., 1980; Xie et al., 2012) and consequently brittle materials are relatively well-characterised compared to ductile materials (Lee et al., 2006; He et al., 2011; Li et al., 2012). However in order to evaluate fracture toughness of ductile materials which exhibit a more complex behaviour, more research is needed to have a robust approach for this type of material. Ductile material indentation behaviour is hence the field of investigation of the present paper. It is analyzed experimentally and is also numerically examined.

Indentation tests can be performed with different types of indenters including spherical, Vickers and Berkovich indenters. Usually spherical indenters are adopted in the tests when the research is aimed at the understanding of elastoplastic behaviour (Xu and Chen, 2010; Ogasawara et al., 2009; Cao and Lu, 2004). However, in this work, in order to have a crack-like structure that allows evaluation of the fracture toughness, a Berkovich indenter which is classified as a sharp indenter, is used. Moreover, in order to be able to assess the fracture toughness obtained by the micro indentation technique, a classical compact tension (CT) test has been performed and the obtained results are compared with the alternative indentation method. Thus a multi-scale approach is used in the present paper comparing a material characterization based on microscopic scale tests with the classical CT tests that belong to the usual mechanical specimens scale.

The multi-scale aspect of the present work can also be appreciated in the theoretical concept used to obtained fracture toughness of the material by means of micro-indentation tests: fracture toughness is evaluated, as usual, on the basis of the fracture energy that is obtained by elaboration of load and displacement thus related to macroscopic quantities. However, as highlighted in the following, fracture energy used in the present work is obtained by indentation deformation. The two quantities are connected through continuum damage mechanics theory thus elastic modulus degradation caused by voids generated beneath the indenter; voids act at a microscale thus is evident the multiscale inferences of the discussed approach.

The research has been carried out on an aluminium alloy. In general, aluminium alloys have good mechanical properties, high corrosion resistance and low density. Nowadays these alloys are widely used in many engineering fields and in particular in contexts in which weight reduction is a critical factor such as in the aerospace and automotive industries. Although pure aluminium is one of the most widespread elements on earth, it is too soft and ductile. It is therefore often combined to form alloys with many different elements, such as copper (Cu), silicon (Si), magnesium (Mg), zinc (Zn) and manganese (Mn). Al6061-T6 belongs to the aluminium series 6000 with silicon and magnesium as the principal alloying components. Such a material is used also in aerospace structures for critical components (Giglio and Manes, 2011); particularly in this case the availability of the fracture toughness performance of the real components (after the whole manufacturing process) is a key requirement.

In indentation methodology, pile-up/sink-in phenomenon is one of the challenges that researches are faced with. Due to the ductility of aluminium alloys, pile-up effect is the case of present paper which affects the contact area between the indenter and the target material and consequently some mechanical properties such as elastic modulus. However, in the present work, the aim is to propose a simple approach to calculate fracture toughness of ductile materials therefore pile-up effect is not considered. Also, Moy et al. (2011) have studied the pile-up effect on the elastic modulus, which is an important parameter in the proposed methodology, in an aluminium alloy and noticed that it can influence this parameter by less than 3%.

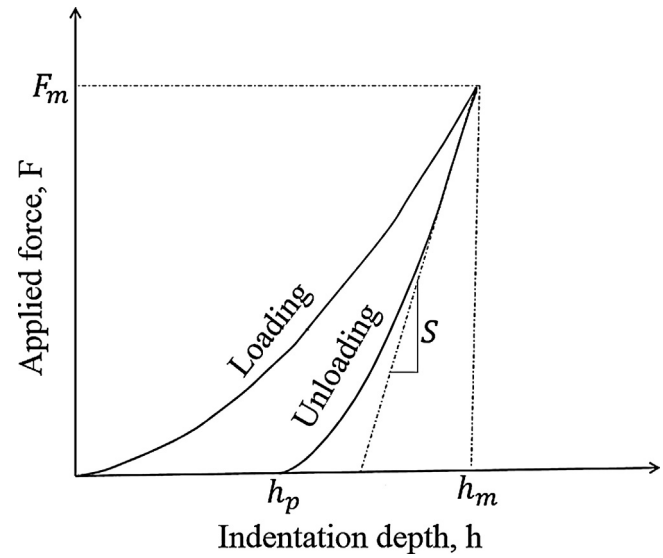

Fig. 1. Indentation load versus indentation depth curve, S is the unloading stiffness.

2. Theoretical concepts

2.1. Identification of the effective elastic modulus

Generally indentation tests can be performed in two modes: force control and depth control. In both modes, applied load and indentation depth are acquired cautiously during the test. A typical single indentation load versus depth curve during loading–unloading is shown in Fig. 1.

Oliver and Pharr (1992) state that the first portion of the unloading curve may not be linear, which is known as the power law method, and can be described by a power law relationship presented in Eq. (1);

$$F = F_m \cdot \left(\frac{h - h_p}{h_m - h_p} \right)^m \tag{1}$$

where m is a constant and can be determined by a fitting procedure.

Therefore, the contact stiffness, which is necessary to calculate the reduced modulus of contact, is evaluated by the derivative at the peak load (Eq. (2))

$$S = \left(\frac{dF}{dh} \right)_{\max} = m \cdot F_m \cdot \left[\frac{(h_m - h_p)^{m-1}}{(h_m - h_p)^m} \right] = m \cdot F_m \cdot (h_m - h_p)^{-1} \tag{2}$$

Considering the fundamental concept of contact mechanics, when two objects (i,ii) are in contact, the indenter and the target material in the indentation test, the relation between the reduced modulus (E_r) of contact and the elastic modulus of the two objects (E_i, E_{ii}) can be expressed as Eq. (3);

$$E_r = \left[\frac{1 - \nu_i^2}{E_i} + \frac{1 - \nu_{ii}^2}{E_{ii}} \right]^{-1} \tag{3}$$

where ν_i and ν_{ii} are Poisson's ratio of the two objects which are in contact.

In indentation tests, where the cross section of the specimen after indentation is shown in Fig. 2, a reduced elastic modulus of contact can be obtained by using unloading stiffness (S), see Fig. 1, a projected contact area (A_c) and β, which is a correction factor for

Table 1
Chemical composition of Al6061-T6.

Component	Al	Mg	Si	Fe	Cu	Mn	Cr	Zn	Ti
Wt. %	98	0.8–1.2	0.4–0.8	0.7	0.15–0.4	0.15	0.04–0.35	0.25	0.15

the indenter due to the lack of axial symmetry, as expressed in Eq. (4);

$$E_r = \frac{S\sqrt{\pi}}{2\beta \quad \overline{A_c(h_c)}} \tag{4}$$

The projected contact area A_c between the indenter and the material is a function of contact depth h_c and this parameter can be calculated theoretically or based on the calibration by the manufacturer of the indentation machine. To achieve precise results the calibrated contact area by the indentation machine manufacturer is considered in this work.

2.2. Indentation energy model

Based on the Griffith theory in an infinite plate, the critical propagation stress depends on the energy per unit area (γ) as well as the crack size and the elastic modulus (Lee et al., 2006). However, this energy parameter is the sum of the surface energy and the plastic deformation energy but the plastic deformation energy is much higher than the surface energy. Therefore, the surface energy in not considered in the present study (Lee et al., 2006). Furthermore, by considering a stress intensity approach and the Griffith theory, the fracture toughness can be expressed as a function of plastic deformation energy (Eq. (5));

$$K_C = \quad \overline{2E\gamma} \tag{5}$$

The fracture toughness in this work is evaluated on the basis of the indentation energy to fracture model. The equation of the indentation energy in expressed (He et al., 2011) as in Eq. (6);

$$\gamma^* = \quad {}_0^{h_p^*} \frac{P(h_p)}{A_p(h_p)} dh_p \tag{6}$$

where A_p is the projective area of the indentation tip due to the unrecoverable plastic deformation. h_p^* is the critical indentation depth corresponding to the representative fracture initiation point which cannot be identified directly from the indentation test. Therefore it is obtained by considering the elastic modulus degradation based on continuum damage mechanics (CDM).

2.3. Identification of the critical indentation depth

Although an indentation test on brittle materials usually generates severe cracks, when a ductile material is tested, the applied load produces an extended plastic deformed zone. Consequently, the evaluation of the critical damage level of the ductile material and the ultimate damage value at failure are difficult to obtain. In order to overcome this difficulty, Lee et al. (2006) proposed an indentation energy to fracture based model that relates the indentation deformation energy to the fracture energy based on continuum damage mechanics (CDM). This model can be used to predict the fracture toughness. In the present work, the elastic modulus degradation technique is followed during the test since Lee et al. showed that during an indentation test voids are generated beneath the indenter therefore the effective elastic modulus is decreased during the test as the indentation depth increases. The elastic modulus degradation technique can be expressed as:

$$D = 1 - \left(\frac{\tilde{E}}{E}\right) \tag{7}$$

where D is the damage variable which can be found by a loading–unloading tensile test (Lemaitre and Dufailly, 1987) and $\tilde{E}$ is the corresponding effective elastic modulus of the damaged material.

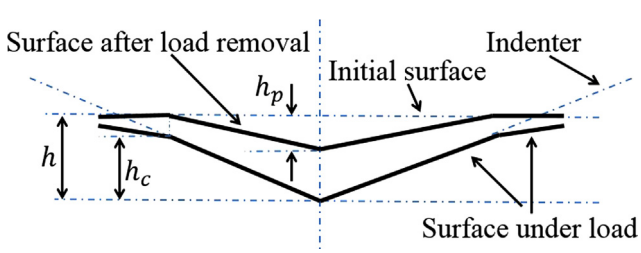

Fig. 2. Cross-section of an indentation test.

3. Experimental tests

3.1. Material

In this work Al6061-T6, with its chemical composition reported in Table 1 is under investigation. The T6 suffix describes the heat treatment applied to the alloy. In particular T6 stands for a two phase treatment based upon the precipitation hardening phenomenon. The T6 treatment results in a large strength with a small reduction of the break elongation. The first step of the treatment involves heating of the aluminium alloy to temperatures of 495–505 °C for about 30 min followed by natural cooling. The second phase is called aging and consists in exposing the material to a temperature of 160 °C for 18 h.

3.2. Compact tension test

The aim of this work is to evaluate the critical fracture toughness by using a new methodology. Verification of the accuracy of the proposed method in finding the fracture toughness by traditional standards is hence compulsory. Therefore, compact tension (CT) tests are performed according to ASTM E399 on Al6061-T6. The specimens used in the CT tests are single-edge-notched, fatigue pre-cracked, standard proportions and tolerances are used to fabricate them (Fig. 3). Side-grooving is applied after pre-cracking to produce nearly straight fatigue pre-crack fronts. In particular, the specimen thickness B is one-half of the specimen width W. Furthermore, the condition in the ASTM E399 regarding crack size a is followed and this parameter is kept nominally between 0.45 and 0.55 times the width W. Values of these parameters for the two test specimens are listed in Table 2. However, in order to have a valid result with regards to the final critical fracture toughness for the first mode loading condition according to this test method, the P_{max}/P_Q requirement should be satisfied; where P_{max} is the maximum force that a specimen is able to sustain. The definition of

Table 2
Important dimensional values for the two compact tension specimens.

	B [mm]	W [mm]	a [mm]
Specimen 1	25.47	50.96	25.448
Specimen 2	25.45	50.86	25.3

Fig. 3. The compact $C(T)$ specimen after the test.

P_Q can be found in the standard (ASTM E 399, 2009). According to this condition, the required ratio should not exceed 1.10. In this work, the P_{max}/P_Q ratio is around 1.30 which does not satisfy the standard requirement and, due to technical limitations such as the fixture design, an increase of the specimen thickness B is necessary to overcome this problem could not be achieved. Therefore, it can be concluded that the critical fracture toughness K_{IC} should be lower than the obtained fracture toughness value K_C in this work. However the obtained fracture toughness results of test are compared with the K_{IC} value obtained from the literature (NASGRO 4.11, 2004; Meyers and Chawla, 2008) and they show a potentially good agreement as shown in Fig. 8.

3.3. Indentation test

The indentation specimen is prepared carefully and polished with silicon carbide abrasive papers up to P1200 and degreased by acetone. The tests are performed by an instrumented micro-indenter (Microcombi Platform-CSM Instruments) with load resolution of 0.3 mN and depth resolution of 0.3 nm. All the tests are carried out with a loading–unloading speed of 300 mN/min to avoid dynamic effects. In this study, the micro-indentations are carried out by using a Berkovich indenter, which is made of diamond. The tests are performed under load control to peak load 200, 400, 600, 800, 1000, 1200, 1400, 1600 mN with a progressively loading–unloading process with keeping the load at each peak for 10 s. All of the tests have been performed under ambient conditions to avoid any noise during the test that could have minor effects on the results.

4. Results and discussion

In the indentation test, the experimental applied load versus indentation depth for the complete loading–unloading process on Al6061-T6 is shown in Fig. 4. The microstructure of the Berkovich indent during the test is shown in Fig. 5. By analyzing the experimental data, the applied load, as a function of the plastic indentation depth, is calculated and illustrated in Fig. 6a. The relation of the applied load and the plastic indentation depth can be described with a power law relationship (Eq. (8)). In order to calculate the indentation energy, the evaluation of the projected area of the indentation tip due to plastic deformation is mandatory. The relation between the projected indentation area and the plastic deformation depth is described in Fig. 6b and the power fit curve (Eq. (8)) expresses their relation similar to the applied load versus plastic depth curve. The power law relation can be expressed as;

$$b = ka^n \tag{8}$$

where the values of the fitted curves are presented in Table 3.

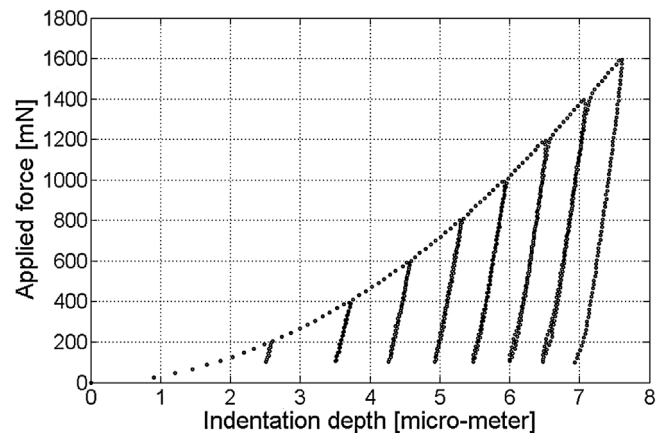

Fig. 4. Applied load versus indentation depth during the indentation test.

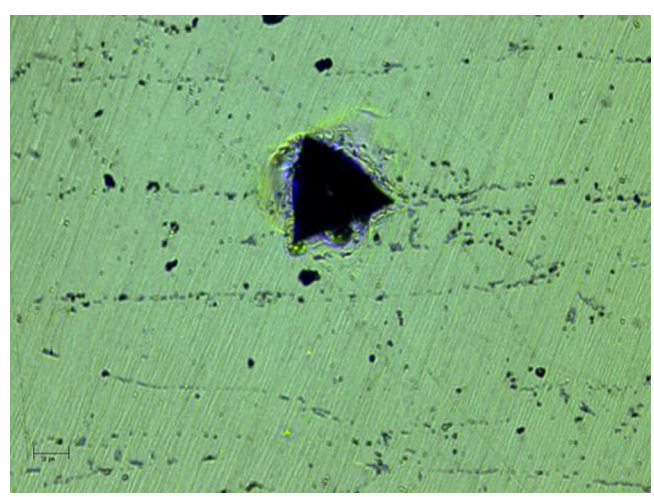

Fig. 5. Microstructure of the Berkovich indent in the indentation test.

Table 3
The power law fitted values of the applied load versus the plastic indentation depth and the projective contact area versus the plastic indentation depth curves.

	k	n
$P(h_p)$	25.65	2.209
$A_p(h_p)$	24.56	2

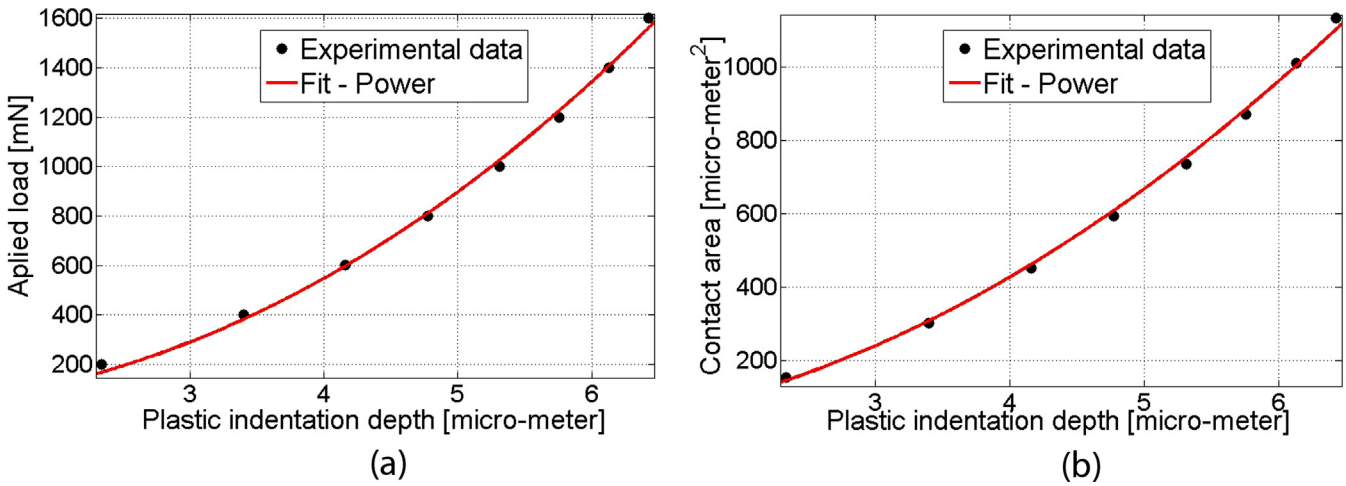

Fig. 6. (a) Applied load versus plastic indentation depth and (b) projected indentation area versus plastic indentation depth during the indentation test.

4.1. Effect of h_p on $\tilde{E}$

The evolution of the effective elastic modulus $\tilde{E}$ during the indentation tests is shown in Fig. 7. The indentation depth increases while the effective elastic modulus of the target material decreases, which reflects the damage accumulation underneath the Berkovich indenter. The obtained effective elastic modulus data from the indentation can be expressed as a function of the plastic indentation depth by using an exponential fitting equation. In this work, in order to find a critical effective elastic modulus $\tilde{E}^*$, the critical damage variable D^* of 0.14 for Al6061-T6 at the fracture point is taken from the literature (Li et al., 2011). Subsequently, based on the elastic modulus degradation technique (Eq. (7)), the critical elastic modulus of this aluminium alloy is 60.2 GPa. Considering the exponential behaviour, which is shown in Fig. 7, the critical plastic indentation depth h_p^* is 8.11 μm.

4.2. Critical energy analysis and identification of K_{IC}

Considering Eq. (6), the critical indentation energy per unit area γ^* is calculated by using the experimental indentation data and the h_p^* obtained in Section 4.1. Finally, the fracture toughness of Al6061-T6 is evaluated through Eq. (5) and the obtained value is 38.9 MPa$\sqrt{\text{m}}$. This K_{IC} value is compared with the values from NASGRO 4.11 (2004) and Meyers and Chawla (2008) and also the experimental compact tension (CT) test results shown in Fig. 8. The K_{IC} value obtained by the indentation methodology is relatively comparable to either of the afore mentioned values, it differs from the NASGRO value by approximately 31% and by 14% from the Meyers and Chawla (2008) value (Table 4). Moreover, in Fig. 8 the trend of K_C is reported according to the NASGRO formulation. According to the NASGRO framework, K_{IC} is a plane strain fracture toughness whereas K_C is any other available fracture toughness. Although the value found during the experimental procedure is not K_{IC}, considering the technical limitation due to the specimen thickness in the CT test, the identified K_C values from CT tests stand in good agreement with the fracture toughness curve of the NASGRO which is the function of the $C(T)$ specimen thickness, thus the experimental CT tests prove that the reference value K_{IC} from NASGRO 4.11 (2004), Meyers and Chawla (2008) are target values also for the material of the present research.

Table 4
The exact value of K_{IC} by different sources and their differences in percentage.

	K_{IC} [MPa$\sqrt{\text{m}}$]	Difference [%]
Present work	38.9	–
Meyers and Chawla (2008)	34	14
NASGRO 4.11 (2004)	29.69	31

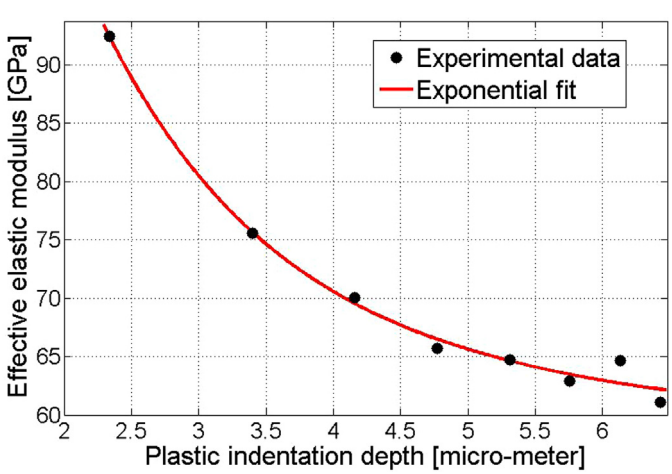

Fig. 7. Effect of the plastic indentation depth on the effective elastic modulus during the indentation test.

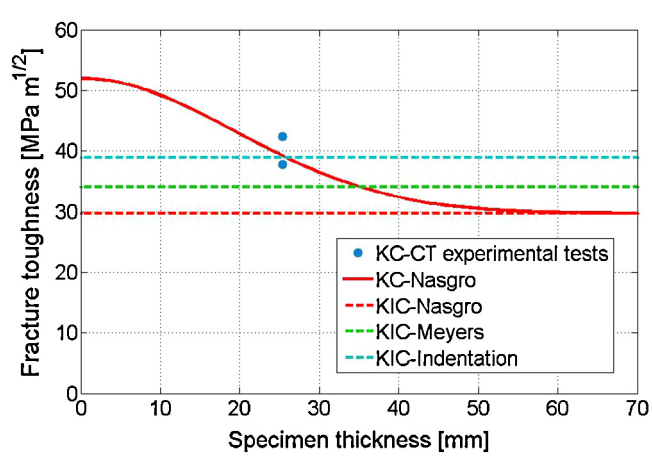

Fig. 8. Comparison of the fracture toughness by different sources.

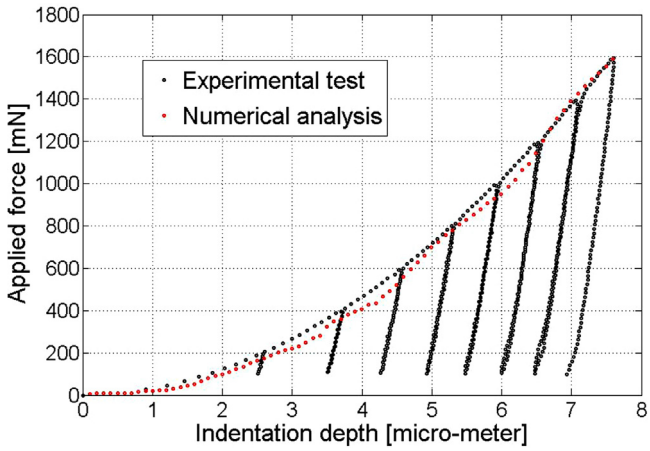

Fig. 9. Comparison between data from experimental tests and results from numerical analysis.

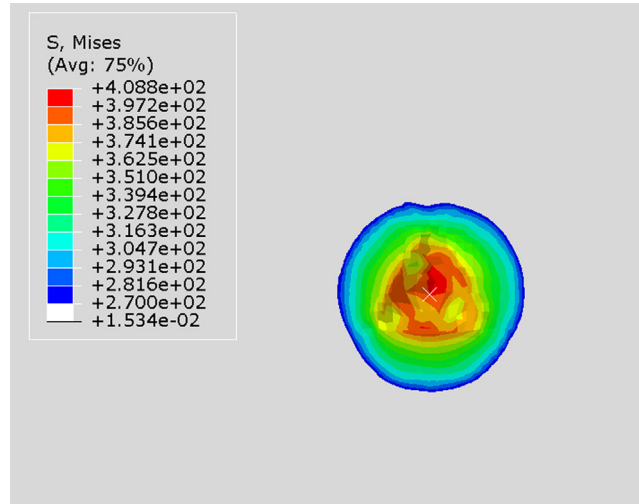

Fig. 10. Von Mises stress distribution [MPa] at applied load 1259 [mN].

4.3. Numerical modeling by using FEM

As already mentioned in the previous section, in order to obtain a crack-like structure in the indentation method that allows the evaluation of the fracture toughness, a Berkovich indenter which is classified as a sharp indenter has been used to have a highly concentrated stress area under the indenter. The commercial software ABAQUS is used to evaluate the stress states in the indentation test. In the numerical analysis, the Johnson–Cook constitutive model (Johnson and Cook, 1985) is adopted to evaluate the plastic behavior; corresponding calibrated constants of this model for Al6061-T6, such as the material elastic limit and the work hardening constant, are obtained from the work of Giloli et al. (2010).

A three dimensional finite element model has been constructed to simulate the indentation process. The target material is meshed using 153,600 eight nodes brick elements, where a finer mesh near the contact region and a gradually coarser mesh further away from the contact region have been designed to ensure accuracy and an efficient simulation in terms of time. The size of the elements in the fine mesh region is $1 \times 1 \times 1\,\mu m^3$. A convergence analysis is performed to check the mesh effect of the FEM model. In the indentation numerical analysis, the Berkovich indenter, which is made of diamond, is assumed as rigid. This assumption significantly decreases the time required by the solver to analyze the indentation process. The analysis has been conducted with an explicit code using quasi-static approach due to the high nonlinear behaviour. Furthermore an energy analysis has been carried out to ensure a quasi-static approach.

Fig. 9 shows a comparison between the indentation load–penetration depth curves from experimental tests and numerical analysis. The similarity is noticeable especially considering that plastic behavior used inside the numerical model has been calibrated from standard tensile tests data. Moreover, the numerical model considers only a single loading step whereas experimental tests have been carried out by means of a loading–unloading procedure. In Fig. 10, an overview of the state of stress around the indented area, corresponding to the applied load of 1259 mN, is reported. It is shown that stress state inside the indented region exceeded the value of 340 MPa. According to the yield stress found in Giloli et al. (2010), 270 MPa, such indentation tests allow to investigate also the behavior of material in presence of high plasticity deformation, where it's expected that ductile failure may modify material behavior also in terms of elastic modulus degradation.

5. Conclusion

An evaluation of the critical fracture toughness of a ductile bulk material by using a non-destructive technique as an alternative for the traditional standard tests, have been carried out by the authors. In this work, precise attention has been paid to the evolution of the effective elastic modulus of the Al6061-T6 target material, during the indentation process. Indentation tests have been performed against Al6061-T6 by using the Berkovich sharp indenter. The stress state of the indentation test has been investigated by using numerical analysis. The fracture toughness of the Al alloy has been evaluated by the standard fracture toughness tests as well to verify the proposed indentation approach. The indentation energy to the fracture model has been used to estimate the fracture toughness. Application of this model requires the identification of the critical plastic indentation depth h_p^* which has been shown to be 8.11 μm. This critical plastic indentation depth h_p^* is obtained by applying the elastic damage degradation theory and the proposed exponential behaviour of the effective elastic modulus as a function of the plastic indentation depth h_p during the indentation test. The fracture toughness obtained from the micro-indentation method of 3.89 MPa$\sqrt{m}$, is compared with values obtained from the consolidated, time-consuming and expensive experimental approach, showing the capability of the method. This method requires only a micro-area to perform the test and thus is very fit for the investigation of minimal amount of material. This approach can furthermore be helpful in the investigation of the fracture toughness of components which exhibit different stress conditions or microstructures along the component. Moreover, by applying this method, it could also be possible to evaluate time dependent as well as temperature dependent material degradation that can occur in the components during operational life in heavy service condition.

References

Ambriz, R.R., Chicot, D., Benseddiq, N., Mesmacque, G., De La Torre, S.D., 2011. Local mechanical properties of the 6061-T6 aluminium weld using micro-traction and instrumented indentation. European Journal of Mechanics, A/Solids 30 (3), 307–315.

ASTM E 399, 2009. Standard Test Method for Linear-Elastic Plane-Strain Fracture Toughness KIc of Metallic Materials. ASTM, Philadelphia, USA.

ASTM E 1820-08, 2008. Standard test method for measurement of fracture toughness. ASTM International.

Cao, Y.P., Lu, J., 2004. A new method to extract the plastic properties of metal materials from an instrumented spherical indentation loading curve. Acta Materialia 52 (13), 4023–4032.

Giannakopoulos, A.E., Suresh, S., 1999. Determination of elastoplastic properties by instrumented sharp indentation. Scripta Materialia 40 (10), 1191–1198.
Giglio, M., Manes, A., 2011. Terminal ballistic effect on the crack growth assessment of a helicopter rotor drive. Engineering Fracture Mechanics 78 (8), 1542–1554, 5.
Giglio, M., Manes, A., Viganò, F., 2012. Numerical simulation of the slant fracture of a helicopter's rotor hub with ductile damage failure criteria. Fatigue and Fracture of Engineering Materials and Structures 35 (4), 317–327.
Gilioli, A., Manes, A., Giglio, M., 2010. Calibration of a constitutive material model for al 6061-T6 aluminium alloy. In: 4th International Conference on Advanced Computational Engineering and Experimenting, ACE-X 2010, Paris, France.
He, M., Li, F., Cai, J., Chen, B., 2011. An indentation technique for estimating the energy density as fracture toughness with Berkovich indenter for ductile bulk materials. Theoretical and Applied Fracture Mechanics 56 (2), 104–111, 10.
ISO/TR 29381, 2008. Metallic Materials – Measurement of Mechanical Properties by Instrumented Indentation Test – Indentation Tensile Properties. ISO, Geneva, Switzerland.
Jang, J., Choi, Y., Lee, Y., Kwon, D., 2005. Instrumented microindentation studies on long-term aged materials: work-hardening exponent and yield ratio as new degradation indicators. Materials Science and Engineering A 395 (1/2), 295–300.
Johnson, G.R., Cook, W.H., 1985. Fracture characteristics of three metals subjected to various strains, strain rates, temperatures and pressures. Engineering Fracture Mechanics 21 (1), 31–48.
Lawn, B.R., Evans, A.G., Marshal, B., 1980. Elastic/plastic indentation damage in ceramics: the median/radial crack system. Journal of the American Ceramic Society 63, 574–581.
Lee, J., Jang, J., Lee, B., Choi, Y., Lee, S.G., Kwon, D., 2006. An instrumented indentation technique for estimating fracture toughness of ductile materials: a critical indentation energy model based on continuum damage mechanics. Acta Materialia 54 (4), 1101–1109.
Lemaitre, J., Dufailly, J., 1987. Damage measurements. Engineering Fracture Mechanics 28 (5/6), 643–661.
Li, H., Fu, M.W., Lu, J., Yang, H., 2011. Ductile fracture: experiments and computations. International Journal of Plasticity 27 (2), 147–180, 2.
Li, J., Li, F., He, M., Xue, F., Zhang, M., Wang, C., 2012. Indentation technique for estimating the fracture toughness of 7050 aluminum alloy with the Berkovich indenter. Materials & Design 40 (0), 176–184, 9.
Luo, J., Lin, J., 2007. A study on the determination of plastic properties of metals by instrumented indentation using two sharp indenters. International Journal of Solids and Structures 44 (18/19), 5803–5817.
Maerky, C., Guillou M., Henshall, J.L., Hooper, R.M., 1996. Indentation hardness and fracture toughness in single crystal TiC0.96. Materials Science and Engineering A 209 (1/2), 329–336.
Meyers, M., Chawla, K., 2008. Mechanical Behavior of Materials, 2nd ed. Cambridge University Press, New York, UK.
Moy, C.K.S., Bocciarelli, M., Ringer, S.P., Ranzi, G., 2011. Identification of the material properties of al 2024 alloy by means of inverse analysis and indentation tests. Materials Science and Engineering A 529 (1), 119–130.
NASGRO 4.11, 2004. Reference Manual, NASA Johnson Space Center.
Ogasawara, N., Chiba, N., Chen, X., 2009. A simple framework of spherical indentation for measuring elastoplastic properties. Mechanics of Materials 41 (9), 1025–1033.
Oliver, W.C., Pharr, G.M., 1992. An improved technique for determining hardness and elastic modulus using load and displacement sensing indentation experiments. Journal of Materials Research 7 (6), 1564–1583.
Takagi, H., Fujiwara, M., Kakehi, K., 2004. Measuring young's modulus of Ni-based superalloy single crystals at elevated temperatures through microindentation. Materials Science and Engineering A 387–389, 348–351, 1-2 SPEC. ISS.
Xie, Y.J., Hu, X.Z., Chen, J., Lee, K.Y., 2012. Micro-indentation fracture from flat-ended cylindrical indenter. Fatigue and Fracture of Engineering Materials and Structures 35 (1), 45–55.
Xu, B., Chen, X., 2010. Determining engineering stress-strain curve directly from the force-displacement curve of spherical indentation test. Journal of Materials Research 25, 2297–2307.
Ye, D., Cha, H., Xiao, L., Xu, X., 2012. A study of fatigue mesoscopic elasto-plastic properties of a nickel-base superalloy by instrumented microindentation measurements. Journal of Nuclear Materials 420 (1–3), 525–536.
Yonezu, A., Chen, X., 2010. Evaluation of elastoplastic properties and fracture strength of thick diamond like carbon film by indentation. Diamond and Related Materials 19 (1), 40–49.
Zhang, T., Feng, Y., Yang, R., Jiang, P., 2010. A method to determine fracture toughness using cube-corner indentation. Scripta Materialia 62 (4), 199–201.